GANIL

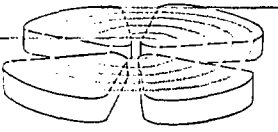

HOT NUCLEI, LIMITING TEMPERATURES

AND EXCITATION ENERGIES

Jean PETER

GANIL, BP. 5027, 14021 Caen-Cedex, France

Invited talk at the International School-Seminar on Heavy Ion Physics, September 1986, Dubna, USSR.

GANIL P. 86-26

HOT NUCLEI, LIMITING TEMPERATURES AND EXCITATION ENERGIES

Jean PETER
GANIL, Caen, France

Abstract : Hot fusion nuclei are produced in heavy ion collisions at intermediate energies (20-100 MeV/U). Information on the maximum excitation energy per nucleon -and temperatures- indicated by the experimental data is compared to the predictions of static and dynamical calculations. Temperatures around 5-6 MeV are reached and seem to be the limit of formation of thermally equilibrated fusion nuclei.

I -INTRODUCTION

Collisions between two pieces of nuclear matter at energies well above the Coulomb barrier provide an unique opportunity of producing nuclear matter in extreme states. At several hundreds of MeV/u, high compressions can be achieved. At intermediate energies, i.e. in the range 20-100 MeV/u, high temperatures in fusion nuclei are expected and have already been measured. The maximum temperatures which can be reached without immediate disruption of the nucleus provide information on the nuclear matter equation of state.

Such hot nuclei are produced in collisions at small impact parameter values (central collisions). At bombarding energies below 10 MeV/u, the behaviour of the system is well defined : all the nucleons from the projectile and target nuclei form a complete fusion nucleus. It recoils in the projectile direction at a fixed velocity. Moreover, a statistical equilibrium between all degrees of freedom is reached, leading to a compound nucleus with a well defined excitation energy. Its nuclear temperature is calculated according to the concept of a Fermi gas. From this well defined state begins the de-excitation through particle evaporation and/or fusion and γ-ray emission. The competition between the different channels is described according to statistical mechanics. The masses, directions and velocities of the residual nuclei are somewhat scattered by these particle emissions, but they remain in a narrow zone which experimentally is well separated from other reaction products.

When the incident energy increases above 10 MeV/u, the situation becomes more and more complicated. Complete fusion is no longer the dominant process in central collisions and vanishes around 25 MeV/u. Incomplete fusion occurs instead. The number of projectile and target nucleons participating into the incomplete fusion nucleus depends on the impact parameter value, resulting in distributions of masses, recoil velocities and directions, and excitation energies. Whether this excitation energy is thermalized will be discussed in this paper. When thermalization is achieved, such nuclei are sometimes called compound nuclei (but this name should be reserved to thermalized complete fusion nuclei) or quasi-compound nuclei, which is an acceptable name.

The excitation energy is large, then many particles are emitted during the de-excitation step, scattering very much the initial directions, mass and recoil velocity, making it difficult to separate fusion nuclei from the products of other reactions.

We will examine in this paper how the residual fusion nuclei are idendified and which information can be obtained about the formation of very excited nuclei, especially the maximum excitation energy or temperature which they can reach. These values will be compared to the maximum temperatures a nucleus can sustain according to several static and dynamical calculations.

II - EXPERIMENTAL METHODS AND RESULTS

The results discussed here have been obtained with projectiles ranging from ^{12}C to ^{84}Kr at energies between 20 and 60 MeV/u. For half of the data, especially these around those around the limiting excitation energies, ^{40}Ar projectiles at energies between 25 and 45 MeV/u have been used, since it was found that fusion vanishes around 35 MeV/u with this projectile.

The used techniques allowed the measurement of the total excitation energy brought in the fusion nucleus or, rather, its excitation energy per nucleon. Direct temperatures measurements are also feasible.

A) MEASUREMENTS OF EXCITATION ENERGIES

1 - The mass-recoil velocity method

Light and medium-mass nuclei de-excite mostly via nucleons and clusters evaporation. The fusion evaporation residues are identified by their mass (or charge), angular direction and velocity. Their mass may not be well separated from the masses of target-like products. Indeed, above ~ 15 MeV/u each projectile nucleon stopped in the target nucleus brings an excitation energy which allows the emission of more than one nucleon : the more complete the fusion, the lower the mass of the evaporation residue, as seen in figure 1[1]. The observed angular distribution $d\sigma/d\theta$ in very broad and peaked at large angles (figure 2). Part of the broadening and deviation from 0° is due to the fusion step and another part is due to the de-excitation step, but it is not possible to disentangle them. Moreover, it is not sensitive to the reaction mechanism : Ar on Ag at 35 MeV/u gives the same angular distribution of heavy residues as at 27 MeV/u, whereas other information show a deep modification of the reaction mechanisms involved.

The only observable which is not modified -on the average- is the recoil velocity $\langle V_R \rangle$. Isotropic emission of evaporated particles scatters V_R around its initial value, so that at an angle θ the distribution of measured recoil velocities is centered at $V_R \cos\theta$. The mass and velocity of the fusion residues and other heavy reaction products are measured via energy-time of flight (fig. I, 2) or radiochemical techniques (γ-ray idendification and range measurements : fig. 3).

For medium-mass and heavy nuclei, fission becomes a widely open de-excitation channel. The same remarks as above apply. The masses of the final fragments can be measured. The angular distribution is washed out by the randomly oriented direction of fission. Again, the recoil velocity value is kept on the average and deduced from the measured correlation angle of the two fission fragments. Indeed, this angle results from the combination of the fisssionning nucleus recoil velocity and the fission velocity (Coulomb repulsion) of the fragments emitted in opposite directions in the center-of-mass of the fissionning nucleus . Since the fission velocity (for symmetric fission) is almost independant of the fissionning nucleus

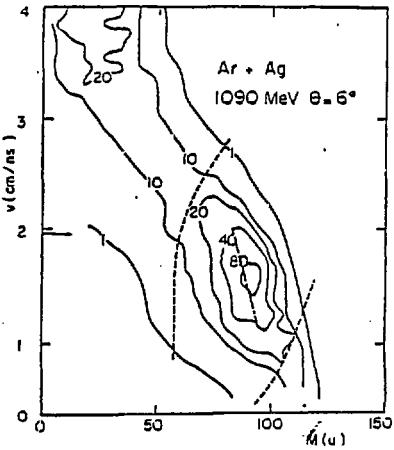

Fig 1 : Mass-velocity diagram of products from Ar collisions on Ag at 27 MeV/u, measured with an energy-time-of flight technique. The arrow is the full momentum transfer velocity. Dashed lines delimitate the region of fusion evaporation residues/1/.

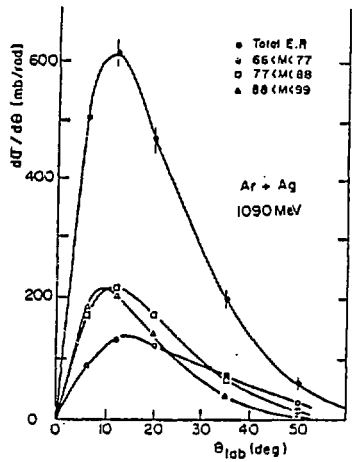

Fig 2 : Angular distribution of evaporation residues for their whole mass range (dashed lines in fig 1) and for selected mass ranges/1/.

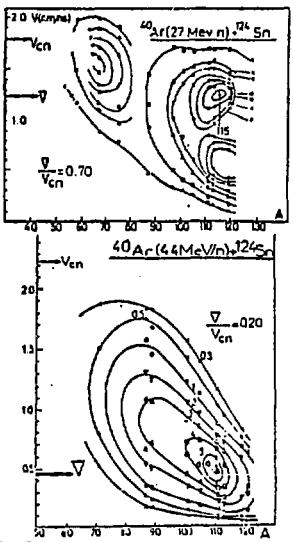

Fig 3 : Mass-velocity diagrams obtained with a catcher-recoil technique at 2 energies. At 27 MeV/u, fusion evaporation residues (top right) are separated from target-like transfer products and fission fragments/3/.

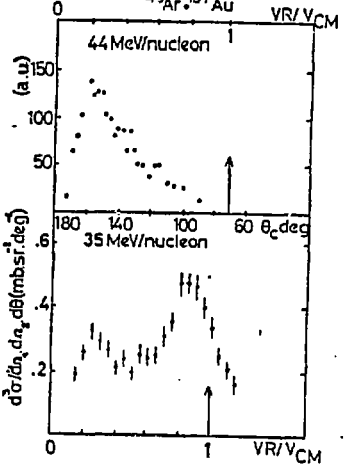

Fig 4 : Angular correlation between coincident fusion fragments produced in reactions of ^{40}Ar on ^{197}Au at 35 MeV/u/2/ and 44 MeV/u/3/. The upper and lower scales show the corresponding recoil velocities relative to the full momentum transfer velocity. An incomplete fusion peak is present at large velocities at 35 MeV/u.

mass along the beta-stability line, a knowledge of this mass is not ecessary to get the correct average laboratory recoil velocity V_R : figure 4.

The recoil velocity is then used to get a value of the excitation envergy per nucleon of the fusion nucleus and sometimes also its total excitation energy E*. Indeed, incomplete fusion can be described in the framework of a participant-spectator model where the spectator nucleons of the projectile keep their initial velocity Vi. Fusion of A'_1 projectile nucleons with A'_2 target nucleons at rest results in a recoil velocity :

$$V_R = A'_1 / (A'_1 + A'_2).Vi \qquad (1)$$

Since A'1 and A'2 are not known, the total excitation energy E* of the system cannot be calculated. It is easily shown, however, that one can obtain the excitation energy per nucleon from the measured V_R and known Vi :

$$\frac{E^*}{A'_1+A'_2} = (Vi - V_R).V_R \qquad (2)$$

if one neglects the reaction mass balance, small compared to the kinetic energy. The evaporation step keeps the value of V_R and (2) is valid to calculate an average value of E*/nucleon.

The value of A'_1 and A'_2 can be estimated, the value of E* is then obtained and an evaporation code is used to calculate the final mass and recoil velocity distributions which are compared to the experimental ones, thus allowing to check the validity of the hypothesis. For symmetric systems, the initial values are easier to get, since A'_1 and A'_2 must be equal.

In the opposite case of asymmetric systems, another assumption was found to be valid : the whole heavy nucleus (i.e. the target nucleus in usual kinematics, the projectile in reverse kinematics) merge with a part of the light nucleus. Then :

$$E^* = A_2 \, . \, Vi \, . \, V_R \qquad (3)$$

E* is proportionnal to the recoil velocity for a given initial system. This is confirmed experimentally in figure 7.

The effects of the de-excitation step on V_R are clearly seen in figures 1, 3 and 4 : velocities larger than that of full momentum transfer are obtained. A careful simulation with an evaporation code should be made in order to extract, for instance, the complete fusion contribution to the fusion cross section (initial $V_R = V_{FMT}$ or V_{CN}). Such an extraction is even more difficult in the case of fission correlation measurements, since an additionnal broadening of V_R is introduced by the mass and kinetic energy distribution of fission fragments[4].

The presence of fusion reactions can be ascertained only when their residues are clearly seen in the mass-velocity diagram (figure 3) or on the fission correlation (figure 4). Then the average velocity of the fusion peak can be used in expression (2) in order to get the average excitation energy per nucleon E*/A of the fusion nucleus. The upper limit of E*/A is obtained at the vanishing of the fusion peak (figure 5). The fast decrease of the fusion cross section as a function of E*/A (or the temperature, see below) helps to get a rather precise determination of E*/A for each system : figure 6.

2 - Coincidence methods

The ideal measurement of E* would require the measurement of all neutrons, charged particles and photons emitted in coincidence with evaporation residues ER or fission fragments FF and their analysis to separate those emitted in the first step of the reaction (not contributing to fusion) from those evaporated from the fusion nucleus during the de-excitation step. Such a complete measurement is not undertaken, to my knowledge. Recent attempts concern neutrons or charged particles.

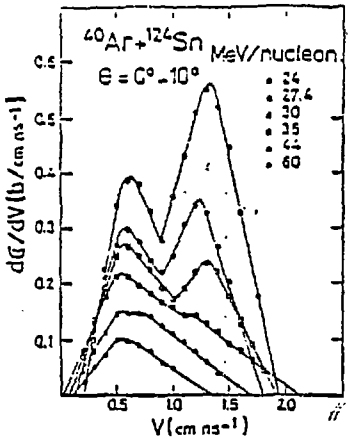

Fig 5 : Velocity distributions of heavy residues (A > 90 in figure 3). The fusion peak is on the right. It vanishes close to 35 MeV/u[57].

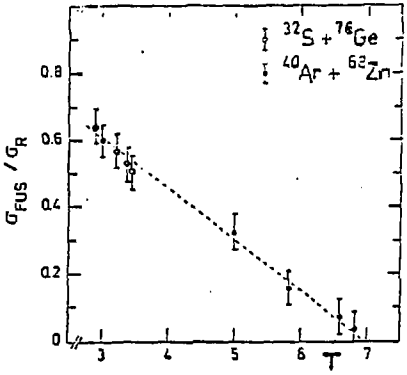

Fig 6 : Ratio of fusion to reaction cross sections as a function of the temperature of the quasi-compound nucleus (incomplete fusion) formed in the $^{32}S + ^{76}Ge$ and $^{40}Ar + ^{62}Zn$ reactions. The broken line is a guide to the eye[67]

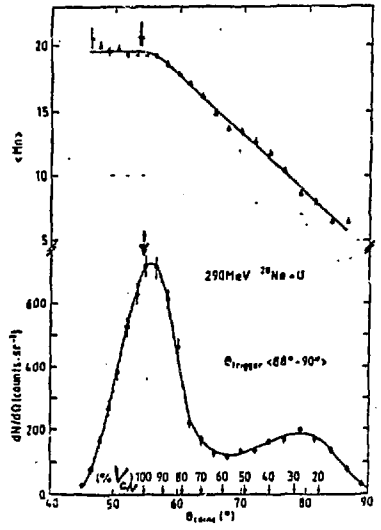

Fig 7 : Bottom : Angular correlations of fission fragments. ^{22}Ne on U at 14.5 MeV/u. The recoil velocity of the fissionning nucleus, V_R, is shown in percentage of the full momentum transfer velocity. Top : number of neutrons detected in coincidence with the fission fragments[77].

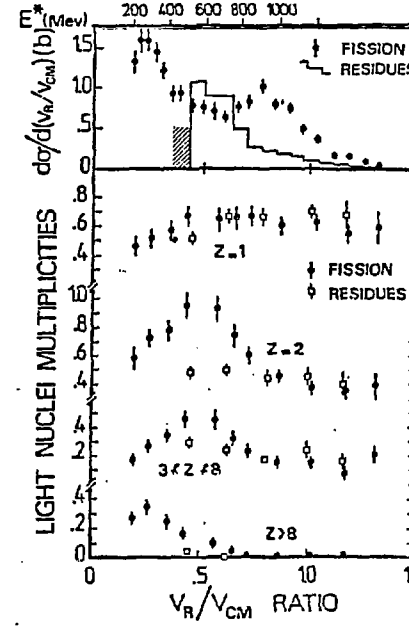

Fig 8 : ^{40}Ar on ^{197}Au at 35 MeV/u. Top : differential cross-sections for the formation of evaporation residues and fission fragments, respectively. Bottom : average multiplicities of light particles and clusters emitted in a forward multidetector (3°-30°) in coincidence with fission fragments or heavy residues[21].

Neutrons carry away a large part of the excitation energy, especially for heavy systems. They have been counted in a nearly 4 π liquid scintillator tank in coincidence with fission fragments : figure 7. The neutron multiplicity increases linearly with the recoil velocity of the fissionning nucleus, as expected from relation (3). Other measurements are in progress with this technique at energies above 20 MeV/u.

Charged particles arrays with a large solid angle can be used in two ways :

- the projectile-like fragments and particles emitted at forward angles are counted in coincidence with ER or FF, thus directly providing the number of projectile nucleons which do not participate in the fusion nucleus ($A_1 - A_1'$ in relation 1). Some evaporated particles are also detected.

- a more complete set-up, nearly 4 π, allows to get all the evaporated charged particles, in order to get E*.

Few experiments have been made. Reactions of Ar at 35 MeV/u on U, Au and Ag nuclei have been studied with forward detector arrays [2, 8, 9]. Complete fusion was shown not to exist anymore, since the ER and FF which seem to be issued from complete fusion ($V_R > V_{CN}$) are found to be in coincidence with one or several nucleons : figure 8. The missing momentum in the fusion nucleus is found in the coincident projectile fragment[11], in agreement with the incomplete fusion picture described above. The kinetic energy spectra of the other particles are consistent with evaporation from incomplete fusion nuclei excited to 700-800 MeV.

B) TEMPERATURE MEASUREMENTS

Measuring a total excitation energy released in a reaction does not necessarily implies that the system had reached a thermal equilibrium. A direct measurement of the temperature eliminates this question. Several methods are available ; most of them have not been applied specifically to fusion nuclei yet.

1 - Kinetic energy distribution of emitted particles

According to statistical thermodynamics, the kinetic energy distribution E of a particle or fragment with binding energy B depends on the temperature T of the heat bath from which it is evaporated :

$$d^2\sigma/d\Omega.dE = C(E-B) \exp - [(E-B)/T] \qquad (4)$$

The high energy part of this distribtion decreases exponentially and the associated slope parameter provides a direct measurement of T. This method has been widely used at low incident energies, where the source of particles is well defined : the compound nucleus. At intermediate energies, a variety of sources has been shown to emit particles. In order to select those emitted from fusion nuclei, a coincidence with the fusion ER on FF is required. An example is given in figure 9 : α-particles have been detected at a backward angle -to minimize the contribution of direct processes- in coincidence with fission fragments emitted at a correlation angle which selects the fusion events (120°-160° for ^{40}Ar on ^{238}U at 27 MeV/u). The high energy slope (4-5 MeV) is consistent with the excitation energy deduced from the recoil velocity.

This method has been applied to the spectra of clusters -or light fragments (3<Z<12)- detected on a broad angular range. If these clusters are emitted from a source with a temperature T and a velocity V_s, and if they are accelerated by Coulomb repulsion, their kinetic and angular distribution can be reproduced with a three parameter fit on T, V_s and the Coulomb repulsion energy. "Apparent temperatures" or slope parameters around 15 MeV are thus obtained for Ar on Ag at 27 MeV/u[11]. Two remarks have to be made :

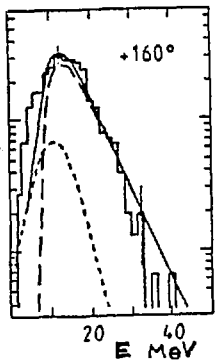

Fig 9 : Kinetic energy distribution of He-particles emitted at 160° (lab.) in coincidence with fission fragments issued from fusion nuclei in the interaction of Ar on ^{238}U at 27 MeV/u[10].

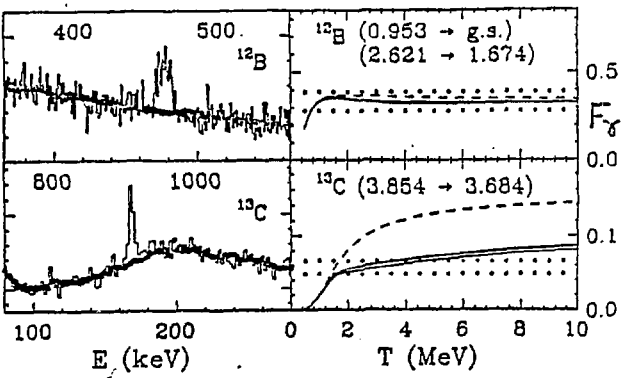

Fig 10 : Left side : γ-ray spectra in coincidence with ^{12}B and ^{13}C fragments, respectively, produced in ^{32}S + Ag reactions at 22.3 MeV/u.
Right side : fractional probability F_γ that an observed fragment is accompanied by the designated γ-ray, as a function of the emission temperature T. Dashed line : calculated assuming no sequential feeding from heavier fragments ; solid lines : sequential feeding included. Dotted lines : range of values for F_γ consistent with the coincidence measurements.

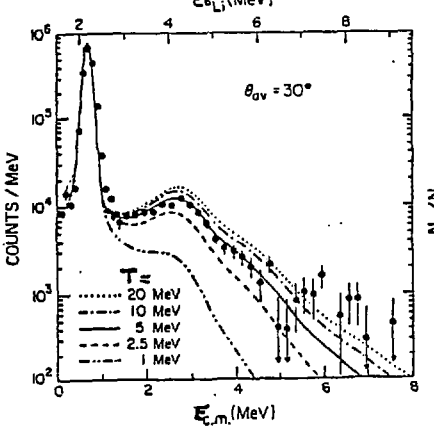

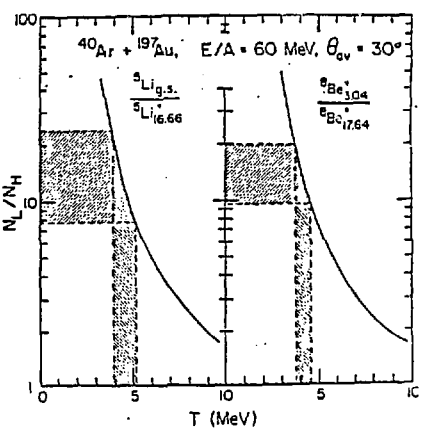

Fig 11 : Left hand side : Relative Energy spectrum resulting from the decay of 2.186 MeV and 4.31 MeV states in ^{5}Li into α + d fragments. The curves correspond to the spectra expected for different emission temperature[17].
Right hand side : Population ratios for two widely separated states in ^{5}Li and ^{8}Be. The solid curve is the calculated ratio as a function of the emission temperature. The hatched regions indicate the range of experimental values including maintainties[18].

1) These sources are not thermally equilibrated fusion nuclei. Coincidence experiments are required to establish the kinetic energy distribution of clusters actually emitted from fusion nuclei.

2) The transformation from slope paremeter to temperature is valid only if the detected clusters are the primary ones. If part of them are issued from sequential decay of excited heavier clusters or fragments, their kinetic energy distribution is broadened by the particle emissions and this looks like a higher temperature spectrum. This effect can introduce an error as large as a factor 2 on the slope parameter /12/.

A temperature value could also be obtained from the slope of the fast photons spectrum emitted from fusion nuclei. Again, no coincidence with fusion nuclei has been made. Only the analysis of inclusive photon spectra emitted in the interaction of Ar on Au at 30 MeV/u and ^{86}Kr on ^{12}C, Ag and ^{197}Au has been carried out /13/. Slope parameters 7.5 and 11 MeV, respectively, have been obtained and are attributed to first collision emission rather than to emission from thermally equilibrated systems.

2 - Relative population of excited states

Not only does the kinetic energy distribution of evaporated clusters depend on T, but also the relative population of their excited states : the probability of producing a state with an energy E_i and a spin j_i depends on T through the Boltzmann factor $\exp[-E_i/kT]$ multiplied by the statistical factor $(2j_i+1)$ which represents the number of magnetic substates. When two levels -upper and lower- are considered, the ratio R of their probalilities is :

$$R = \exp[(El-Eu)/kT] \quad \frac{2ju+1}{2jl+1} \qquad (5)$$

Provided these states are not fed from higher lying states of more massive clusters which undergo particle decay, the measurement of R provides a direct measurement of T /15/.

Depending on the nature of the decay of these excited levels (photon or particle emission), two different techniques have been used :

γ-ray-fragment coincidence method - When the upper level decays to the lower level through γ-ray emission, this γ-ray is detected in coincidence with the cluster and one can obtain the fractionnal probability of γ-ray emission relative to the production of this cluster :

$$F_\gamma = R/(1 + R) \qquad (6)$$

This method has been sucessfully checked on ^{10}B and ^{7}Be fragments emitted from ^{26}Al compound nuclei formed in the interaction of ^{14}N with ^{12}C below 10 MeV/u, i.e. at $T < 1.5$ MeV /14/. Applied to similar fragments (^{6}Li, ^{7}Be...) emitted in the interaction of ^{14}N with Ag at 35 MeV/u and decaying through photon emission, F_γ provided much lower T values ($T < 1$ MeV) than deduced from the slope parameter of the kinetic energy distribution of these fragments ($T = 8 - 10$ MeV) /15/. This contradiction was puzzling. Recently, always for similar fragments produced in ^{32}S reactions on Ag at 22 MeV/u, F_γ has also been measured and compared to the predictions from a quantum statistical model which included sequential feeding from particle unbound states of heavier fragments. This calculation shows that, for $T > 2$ MeV, F_γ is more sensitive to sequential feeding than to the temperature of the emitting system : figure 10 /16/. The deduced temperature is too low. On the other hand, for the same reason, the slopes at high energy of the kinetic energy spectra are modified as explained in II-1, and the deduced T-values are too high.

One can conclude that this method is valid at low temperatures only.

Particle decay - In order to reduce the effect of possible sequential feeding, higher excited levels have to be studied. Since their decay scheme is very complicated, the γ-ray-fragment coincidence method above can no longer be used. When these levels are particle-unbound, the decay particles have to be detected in coincidence and their relative kinetic energy measured with a good accuracy in order to determine the fragment level. Such precise measurements have been performed on clusters produced in ^{40}Ar induced-reactions on ^{197}Au at 60 MeV/u[17 18] and are shown in figure 11. Like for photon decay, the larger the difference of excitation energy ($E_u - E_l$), the less sensitive the ratio R to sequential feeding and the more accurate the T-value : ^{6}Li decays from 2.1 and 4.3 MeV levels give a large error (T = 5 ± 2 MeV), whereas 15 MeV differences between levels for ^{5}Li and ^{8}Be fragments allow to get an accurate value : T = 4.5 ± 0.5 MeV

The relative population of excited states is a powerful method of measuring a temperature. In the examples given above, there was no selection on the reaction mechanism which is responsible for the productions of the light fragments which temperature has been measured. At least they show that a temperature around 5 MeV is reached in the emission system, which is likely a fusion nucleus or a multi-fragmenting system obtained in central collisions (see III-C). A more definite conclusion would require a coincidence with fusion residues or fission fragments, or the detection of the other multifragmentation products.

C) MAXIMUM EXCITATION ENERGY PER NUCLEON IN FUSION NUCLEI

As stated in II-A, the excitation energy per nucleon E*/A is the quantity most directly obtained from the experiments made until now. The data obtained by means of the mass-recoil velocity method are collected in figure 12, borrowed from[19], together with few data obtained via other metods. Fusion nuclei are not observed above E*/A = 6 MeV for light systems down to ~ 3 MeV for heavy systems. Most of these limiting values have been obtained with Ar projectiles. Going from E*/A to the temperature T just require to use the constant level density parameter a = A/8 MeV^{-1} i.e. $E^*/A = T^2/8$. The right hand side scale shows the T-values obtained with this formula, in order to facilitate a comparison with the theoretical predictions on T. a = A/8 is the value given by low temperature data and generally used. Thomas-Fermi and Hartree-Fock calculations confirm the linear mass dependence of a, but give a value close to A/13. With this value, the T scale in figure 12 would be multiplied by a factor 1.27.

Is this transformation from E*/A to T valid, i.e. is thermalization achieved ? The mass-velocity distributions are in agreement with the predictions of statistical de-excitation codes based on this assumption[20]. The other methods support a positive answer to this question. Figure 7 provides a strong indication that E* is thermalized, but here T does not exceed 3 MeV. Higher temperatures have been measured in a few coincidence measurements or in direct temperature measurements : thermalization seems to be achieved and fusion nuclei formed up to a temperature ~ 5 MeV, at least.

III - PREDICTED LIMITING TEMPERATURES OF NUCLEI

The simplest idea about the maximum excitation energy per nucleon that a nucleus can sustain is to make it equal to the average binding energy of its constituent nucleons, i.e. around 7-8 MeV. A nucleus formed at a higher excitation energy would split into many nucleons and clusters and no main residue or pair of fission fragments could be observed. The decrease of E*/A as a function of A in figure 12 reflects the behaviour of the binding energy per nucleon with A above 50, but the absolute values are not reproduced. Let us examine the theoretical estimations of the limiting temperatures of nuclei. The static and dynamical

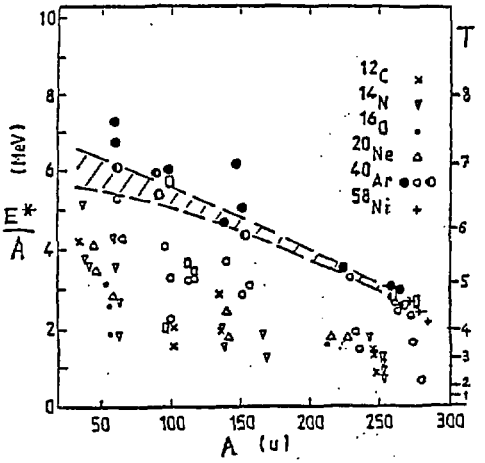

Fig 12 : Excitation energy per nucleon, E*/A, deposited in a fusion nucleus of mass A : open points. The black points correspond to systems where no fusion could be observed (then, E*/A is calculated assuming a transferred linear momentum per projectile nucleon : 175 MeV/c). The dashed area indicates the region where E*/A seems to reach its limiting value. From /19,6/. Rectangles, from /10,12,35/

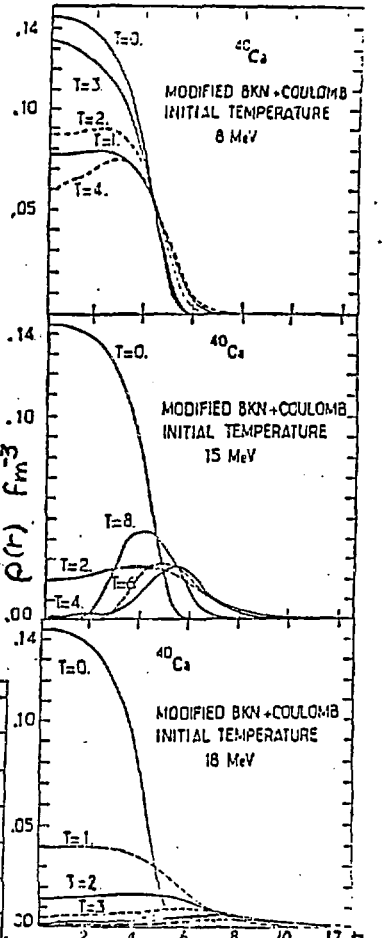

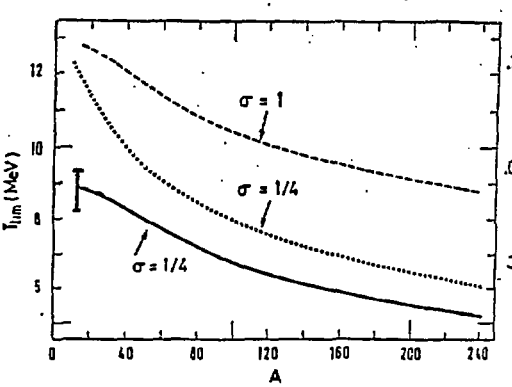

Fig 13 : Calculated maximum temperature of nuclei along the beta-stability line. $\sigma = 1/4$ corresponds to a compressibility factor deduced from experimental results : K = 222 MeV ; the solid line is obtained assuming a quadratic variation of the surface tension with the temperature, and the dotted line a linear variation. $\sigma = 1$ means a very large K-value : 384 MeV /24/

Fig 14 : Profile densities as a function of time T in 10^{-22}s units of ^{40}Ca initially heated without size change nor compression /29/.

calculations described below do not deal with the question of whether such nuclei could have been formed. Possible limitations in the formation, as well as the transition to multifragmentation, are briefly discussed.

A) STATIC CALCULATIONS

They assume that, in the first stage of the reactions, the single particle degrees of freedom have been thermalized and that the radius of this excited quasi-compound nucleus is that of the cold nucleus : that can be called the "sudden heating assumption". This isolated hot nucleus is a metastable system which decays by particle emission. These particles form a vapor around the dense (liquid) nucleus and the stability of the nucleus is related to the possibility of coexistance between a liquid and a gas phases of nuclear matter[21 22]. Indeed, for infinite neutral nuclear matter, the phase diagram exhibits the structure of a Van der Waal's fluid : an equilibrium between liquid and vapor phases is possible below the critical temperature Tcr. Tcr is around 20 MeV for Hartree-Fock calculations with a Skyrme III force[23].

In the framework of the hot liquid drop model, the status of the system is obtained by mininizing the total free energy in the nucleus and the surrounding vapor versus the volume of the nucleus and its number of nucleons. This leads to coexistence equations based on equal pressures and chemical potentials in both phases. An equation of state has to be chosen, as well as the variation of the surface tension with T. Numerical applications with 16 and 24 MeV for the binding and kinetic energies per nucleon, 0.17 fm^{-3} for the saturation density and 222 MeV for the compressibility factor lead to Tcr = 18 MeV in infinite nuclear matter. For a realistic nucleus, finite size, surface and Coulomb effects have to be taken into account. The addition of a surface term in the coexistence equations increases the stability, since the internal pressure can increase ; Tcr is unchanged. But Coulomb repulsive forces have the opposite effect, and the coexistance equations reach the limit of the liquid phase at a temperature much lower than Tcr. This value is called Tlim or flash-temperature and varies with the charge-to-mass ratio of the system. For nuclei not far from the beta-stability line, Tlim decreases with increasing A (figure 13), thus reproducing the trend observed in figure 12. The absolute values depend on the choice of parameters. In figure 14, the more realistic choice (solid line) is in rather good agreement with the data.

Calculations in the same spirit of liquid-vapor equilibrium have been made in the mean field approximation of the Hartree-Fock framework[24]. Tlim value is always slightly smaller than the temperature at which the nucleus binding energy vanishes. It depends on the effective interaction used in the calculation : for ^{208}Pb, 11 MeV with Skyrme III and 8 MeV with the force SKM.

In a different approach[25] considering that the evaporated particles do not provide an outside pressure, the nucleus is treated like a superheated liquid drop. Tlim for which this metastable nucleus is still bound amounts to 7-8 MeV for ^{208}Pb.

B) DYNAMICAL CALCULATIONS

Several variants to the dynamical mean field approach have been used recently and are listed in[26] : the constrained Hartree-Fock method[27], the time-dependent Thomas-Fermi (TDTF) approximation[28], the Vlasov equation[29], the Monte-Carlo Hartree-Fock method[30] and the time-dependent Hartree-Fock (TD HF) method[26]. We will just extract some general information from them.

Again the sudden heating assumption is used. The nucleus has no compression apart from that resulting from the heating, since its equilibrium density profile

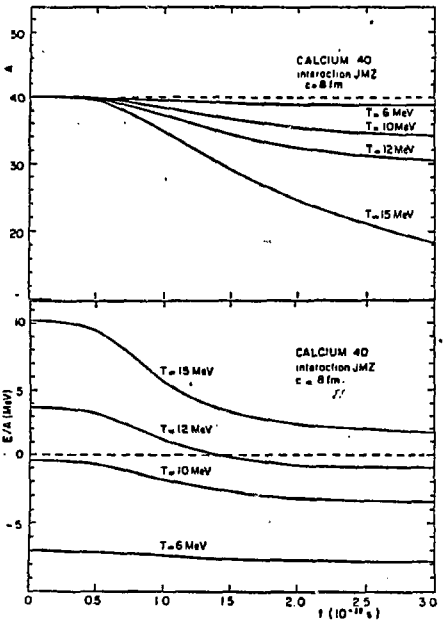

Fig 15 : Time evolution of the excitation energy per nucleon and the mass of the residual nucleus for several initial temperatures, in TDHF calculations/26/.

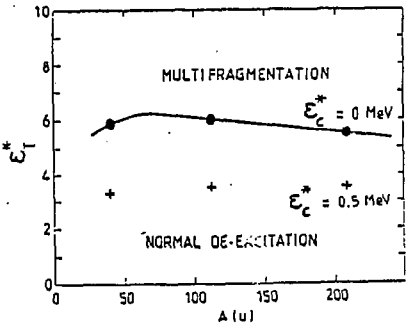

Fig 17 : Maximum thermal excitation per nucleon above which a nucleus undergo multifragmentation, calculated for Ca, Sn and Pb. Black points : without initial compression. Crosses : with an initial compression energy per nucleon equals to 0.5 MeV /32/.

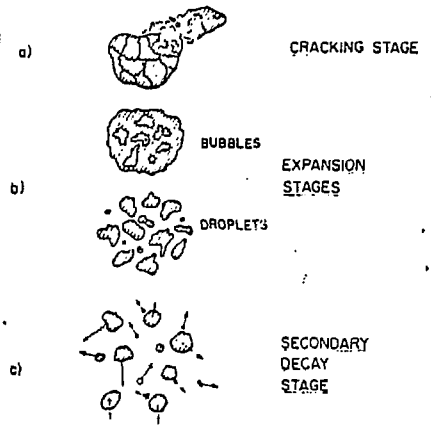

Fig 16 : Schematic view of the fragmentation process : (a) creation of cracks in the initial stage ; (b) formation of fragments during the expansion stage ; (c) evaporation of fragments after the breakup of the composite system /31/.

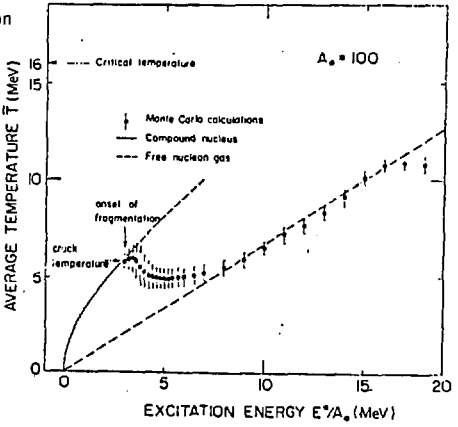

Fig 18 : Average temperature of clusters produced in a nuclear system of mass 100 as a function of the initial excitation energy per nucleon. Below the onset of fragmentation, only one cluster -the compound nucleus- is formed : solid line ; above 8 MeV/u the free nucleons gas limit is reached : dashed line /31/

at a finite T is more extended than in the ground state and it will expand. Evolution equations describe the expansion of this nucleus in a large "box" (the nucleus is always ^{40}Ca, for saving computation time !).

In figure 14, the density profile is displayed at different times for several initial temperatures. In this specific calculation, made by solving the Vlasov equation and using a modified BKN force, the flash T is 18 MeV[29]. At this temperature, the profile continously evolves to a smaller density filling up the box : complete vaporization of nuclear matter occurs. Well below, at 8 MeV, the density oscillates around half the saturation value within the initial volume and the radius fluctuates (breathing mode) and slowly increases with time. Several nucleons have escaped the nucleus and form a low density tail. At T = 15 MeV, the size increase is large and a bubble nucleus is formed ; many particles have escaped at large distances, but nevertheless some residue would remain. In TDHF calculations, the radius and mass of the residual nucleus stabilizes in a few 10^{-22}s at T below 12 MeV. Above 12 MeV, a total vaporization occurs (figure 15), since the energy per nucleon remains positive, the mass of the nucleus continously decreases and its radius increases.

These T_{lim} values are higher than the binding energy per nucleon, but they should not be taken too seriously, since they may be due to the parameter values or to artificial constraints. For instance, a larger value of the compressibility factor, or an effective force which implies it like the BKN force, produces a large value of Tlim (fig. 13) ; the imposed spherical symmetry allows the formation of bubble nuclei which actually would be unstable and split into several fragments.

In the initial stage of formation of the excited nucleus in a heavy ion collision, some energy must be stored into compression. In[28], the effect of this compression is studied by adding a constraining field λr^2 to the mean field. For a large value of λ (2 MeV.fm^{-2}) the expansion is fast and a bubble nucleus would be formed : compressionnal energy is more efficient for breaking nuclei than thermal energy. More precisely, stability will be lost at a smaller total excitation energy if part of it is initially stored in the form of compression (although it decreases the temperature value).

It must be kept in mind that these calculations deal only with the expansion phase. If, at the end of this expansion, a fraction of the nucleons is left in the dense phase, de-excitation of this nucleus goes on until a cold residue is obtained, which mass can be very low.

C) ONSET OF MULTIFRAGMENTATION

Another approach is to allow the sudden disassembly of nuclear matter at any stage of the expansion process[31 32]. This process can be pictured as in figure 16[31] : the matter density decreases until cracks appear in the volume, fragments are formed which no longer interact with each other, then de-excite.

Cracking can be obtained via a percolation model : the nucleus is taken as a lattice initially filled up. Empty sites can appear and bonds can be broken in two ways :

1) Sudden Evaporation percolation. At T ~ 5 MeV, nucleons are evaporated in ~ 10^{-22}s, creating empty sites which remain free if the relaxation time is larger than a few 10^{-22}s[33].

2) Expansion percolation. If the relaxation time is short enough, the system reorganize between successive evaporations and maintain the statistical equilibrium. Thus, empty sites appear not because of evaporated nucleons, but mainly because of expansion : clusters of nucleons become isolated. Following the evolution with time-dependant Thomas-Fermi calculations, several predictions have

been made[32]. For our question of limiting temperature, results are given in figure 17. When there is no compresssion, the maximum excitation energy per nucleon lies around 5.5 MeV (actually, 0.71 times the binding energy B, just because the strength of bonds has been taken to be proportionnal to B). Again, compresionnal energy is found to be more efficient than thermal energy in causing disassembly, since a compression of 0.5 MeV/A brings E*thermal/A down to ~ 3.3 MeV. Taken at face value, the total is E*/A = 3.3 + 0.5 = 3.8 MeV. A comparison to the measured total E*/A in figure 12 would imply some compressionnal energy in central collisions on heavy nuclei (E*/A experimental < 4 MeV). Higher experimental E*/A values for lighter nuclei would mean no compression, which could be explained by an easier sideway flow of nuclear matter during the collision, thus reducing the compression.

The evolution of the system after cracking has been followed taking into account the mass distribution of initial fragments[31]. An interesting feature is, shown in figure 18 : above the crack temperature (~ 6 MeV), multifragmentation occurs and the nascent clusters can move into the larger volume which is then accessible. Some excitation energy is then transformed into translationnal energy and the overheated system cools down. The temperature of these clusters remains in the vicinity of 5 MeV. Experimentally, in the interactions of ^{40}Ar on ^{197}Au at 60 MeV/u, fusion is no longer present and multifragmentation is expected to occur. Temperatures around 4.5 MeV have been measured for light fragments (figure 11) and are in agreement with the above value.

D) LIMITS TO THE FORMATION OF HOT NUCLEI

In an actual heavy ion collision, the additionnal question is whether limitations in the entrance channel could hindrance the formation of a nucleus at the limiting temperature.

Some answer to this question can be found in the dynamical calculations above. The cooling of hot nuclei is very fast. For instance in[26] 4 nucleons are emitted from ^{40}Ca heated at T = 10 MeV in 1.5 10^{-22}s. This number is even larger in[27]. Also, statistical mechanics predict very short times for the evaporation of nucleons : 2.10^{-18}s at T = 1 MeV, 10^{-20}s at 2 MeV, but only 10^{-21}s at 3 MeV and 1.3 10^{-22}s at 5 MeV ! On the other hand, the energy relaxation in a nucleus cannot propagate faster than the sound velocity in nuclear matter (c/5 to c/4), i.e. more than 1.5 10^{-22}s is necessary for the formation and thermalization of the quasi-compound nucleus. During this time, nucleons are evaporated, cooling the system and preventing it to reach a temperature very close to Tlim.

For very heavy nuclei, the question of stability against deformation arises. Shell effects which contribute to the fission barrier height vanish at T above 2 MeV. The liquid drop fission barrier also decreases. Indeed, at high temperature, the equilibrium shape is reached for a larger radius and a more diffuse edge. The volume enlargement leads to a decrease in the Coulomb energy Ec, whereas diffuseness decreases the surface tension and surface energy Es. Es decreases faster with T than Ec and the fissility $x = Ec/2\,Es$ increases[34]. The fission barrier of ^{240}Pu vanishes around T = 4.5 MeV. However, this is not a limit to the formation of such a hot nucleus, since the collective elongation up to the scission point requires a time much larger than the relaxation time of the interval degrees of freedom. This situation is similar to vanishing of the fission barrier due to a very high angular momentum at lower incident energies, which however does not prevent the system to fuse, equilibrate its temperature and undergo quasi-fission.

IV - CONCLUSION

Available experimental data show that thermalized fusion nuclei are formed up to excitation energies around 6 MeV at A ~ 50 down to 3 MeV for very heavy nuclei. More exclusive experiments are needed, where all charged particles in a reaction would be detected, in order to get a more precise value of the limit to incomplete fusion and to observe the onset of multifragmentation.

The observed trend of E*/A is reproduced by static and dynamical calculations on the limiting temperatures nuclei can sustain. Comparing these predictions to the experimental limits will provide information on the parameters which enter in the equation of state of hot nuclear matter.

REFERENCES

1 - M.F. Rivet, P. Borderie, H. Gauvin, D. Gardès, C. Cabot, F. Hanappe, J. Péter, report IPN Orsay. DRE-86-10, submitted to Phys. Rev. C.

2 - G. Bizard, R. Brou, H. Doubre, A. Drouet, F. Guilbault, F. Hanappe, J.M. Harasse, J.L. Laville, C. Lebrun, A. Oubahadou, J.P. Patry, J. Péter, G. Ployart, J.C. Steckmeyer, B. Tamain.
Nucl. Phys. A 456 (1986) 173.

3 - A. Lleres, J. Blachot, J. Crançon, A. Gizon, H. Nifenecker.
Z-Phys A312 (1983) 177.

4 - J.M. Alexander, E. Duek, L. Kowalski.
Preprint SUNY Stony-Brook (1985).

5 - A. Lleres, J. Crançon, J. Blachot, A. Gizon, H. Nifenecker.
Contribution to conference on heavy ion nuclear collisions in the Fermi energy domain, Caen, May 1986, P. 50.

6 - A. Fahli, J.P. Coffin, G. Guillaume, B. Heusch, F. Jundt, F. Rami, P. Wagner, P. Fintz.
Report CRN Strasbourg PN 86-12, april 1986.

7 - G. Ingold, D. Hilscher, U. Jahnke, J. Galin, M. Lehmann, H. Rossner, E. Schwinn, P. Zank.
HMI-Berlin, report nr 429,P. 67 (1985).

8 - G. Bizard, R. Brou, H. Doubre, A. Drouet, F. Guilbault, F. Hanappe, J.M. Harasse, J.L. Laville, C. Lebrun, A. Oubahadou, J.P. Patry, J. Péter, G. Ployart, J.C. Steckmeyer, B. Tamain.
Z.Phys.A 323 (1986) 459.

9 - Y. Patin, S. Levay, E. Tomasi, O. Granier, C. Cerruti, J.L. Charvet, S. Chiodelli, A. Demeyer, D. Guinet, C. Huneau, P. Lhenoret, J.P. Lochard, R. Lucas, C. Mazur, M. Morjean, C. Ngo, A. Péghaire, M. Ribrag, L. Sinopoli, T. Suomijarvi, J. Uzureau, L. Vagneron.
Nucl. Phys. A457 (1986) 146.

10 - D. Jacquet, J. Galin, B. Borderie, D. Gardès, D. Guerreau, M. Lefort, F. Monnet, M.F. Rivet, X. Tarrago, E. Duek, J. Alexander.
Report IPN Orsay, DRE-85-09, submitted to Phys. Rev.

11 - B. Borderie, M.F. Rivet, C. Cabot, D. Fabris, D. Gardès, H. Gauvin, F. Hanappe, J. Péter.
Z-Phys. A 318 (1984) 315.

12 - W. Mittig. Report GANIL P85-13.

13 - H. Nifenecker, M. Kwato Njock, M. Maurel, E. Monnand, J. Pinston, F. Schussler D. Barnéoud, C. Guet, Y Schutz.
Proc. XXIV Meeting on Nuclear Physics, Bormio (1986) p. 239.
14 - D.J. Morrissey, C. Bloch, W. Benenson, E. Kashy, R.A. Blue, R.M. Ronningen, R. Aryaeinejad.
MSU Cyclotron Laboratory report MSUCL-554 (1986).
15 - D.J. Morrissey, W. Benenson, E. Kashy, B. Sherrill, A.D. Panagiotou, R.A. Blue R.M. Ronningen, J. Van der Plicht, H. Utsunomiya.
Phys. Lett. 148 B (1984) 423.
16 - H.M. Xu, D.J. Fields, W.G. Lynch, M.B. Tsang, C.K. Gelbke, D. Hahn, M.R Maier, D.J. Morrissey, J. Pochodzalla, M. Stöcker, D.G. Sarantites, L.G. Sobtka, M.L. Halbert, D.C. Hensley.
Preprint MSUCL-560 (1986).
17 - J. Pochodzalla, W.A. Friedman, C.K. Gelbke, W.G. Lynch, M. Maier, D. Ardouin, H. Delagrange, H. Doubre, C. Grégoire, A. Kyanowski, W. Mittig, A. Péghaire, J. Péter, F. Saint-Laurent, Y.P. Viyogi, B. Zwieglinski, G. Bizard, F. Lefebvres, B. Tamain, J. Québert.
Phys. Rev. Lett. 55 (1985) 177.
18 - J. Pochodzalla et al. Phys. Lett. 161 B (1985) 275.
19 - S. Leray.
Proceedings HICOFED, J. de Phys. Suppl. 47, C4 (1986) 275, and references therein.
20 - G. Auger, D. Jouan, E. Plagnol, F. Pougheon, F. Naulin, H. Doubre, C. Grégoire. Z-Phys. A 321 (1985) 243.
21 - S. Levit, P. Bonche.
Nucl. Phys. A 437 (1985) 426.
22 - E. Suraud. Contribution to HICOFED, p. 68 (1986)
E. Suraud, D. Vautherin. Phys. Lett. 138B (1984) 325.
23 - G. Sauer, H. Chandra, V. Mosel. Nucl. Phys. A 264 (1976) 221.
24 - P. Bonche, S. Levit, D. Wautherin. Nucl. Phys. A 427 (1984) 278. Nucl. Phys. A 436 (1985) 265.
25 - M. Brack, C. Guet, H.B. Hakansson. Phys. Reports 123 (1985) 275.
26 - D. Bonche, D. Vautherin, M. Véneroni.
Proceedings HICOFED, J. de Phys. Suppl. 47, C4 (1986) 339.
27 - H. Sagawa, G.F. Bertsch. Phys. Lett. 155 B (1985) 11.
28 - J. Nemeth, M. Barranco, C. Ngô, E. Tomasi. Z.Phys. A 320 (1985) 691.
29 - L. Vinet, F. Sebille, C. Grégoire, P. Schuck. Preprint GANIL 86-01
30 - J. Knoll, B. Strack. Phys. Lett. 149 B (1984) 45.
31 - J.P. Bondorf, R. Donangelo, I.N. Mishustin, C.J. Pethick, H. Schulz, K. Sneppen. Nucl. Phys A 443 (1985) 321.
J. Bondorf, R. Donangelo, I.N. Mishustin, H. Schulz.
Nucl. Phys. A 444 (1985) 460.
H.W. Barz, J.P. Bondorf, R. Donangelo, I.N. Mishustin, H. Schulz.
Nucl. Phys A 448 (1986) 753.
J. Bondorf, J. de Phys. Suppl. 47 C4 (1986) 263.
32 - J. Nemeth, M. Barranco, J. Desbois, C. Ngô. Preprint CEN Saclay DPh-N-2375 (1986).
33 - J. Desbois, O. Granier, C. Ngô.
Preprint IPN Orsay TH 86-52 (1986).
34 - F. Bartel, P. Quentin.
Phys. Lett. 152 (1985) 29.
35 - R.J. Charity, M.A. Mc Mahan, D.R. Bowman, Z.M. Liu, R.J. Mc Donald, G.J. Wozniak, L.G. Moretto, S. Bradley, W.G. Kehoe, A.C. Mignerey, M.N. Namboodiri, Phys. Rev. Lett. 56 (1986) 1354.